HHS Public Access

Author manuscript

Nat Struct Mol Biol. Author manuscript; available in PMC 2010 October 01.

Published in final edited form as:

Nat Struct Mol Biol. 2010 April ; 17(4): 459–464. doi:10.1038/nsmb.1786.

Spinophilin directs Protein Phosphatase 1 specificity by blocking substrate binding sites

Michael J. Ragusa[1,2], **Barbara Dancheck**[1], **David A. Critton**[2], **Angus C. Nairn**[3], **Rebecca Page**[2], and **Wolfgang Peti**[1]

[1] Department of Molecular Pharmacology, Physiology and Biotechnology, Brown University, Providence, RI, 02912

[2] Department of Molecular Biology, Cell Biology and Biochemistry, Brown University, Providence, RI, 02912

[3] Department of Psychiatry, Yale University School of Medicine, New Haven, CT 06508

Abstract

The serine/threonine Protein Phosphatase 1 (PP1) dephosphorylates hundreds of key biological targets. PP1 associates with ≥200 regulatory proteins to form highly specific holoenzymes. These regulatory proteins target PP1 to its point of action within the cell and prime its enzymatic specificity for particular substrates. However, how they direct PP1's specificity is not understood. Here we show that spinophilin, a neuronal PP1 regulator, is entirely unstructured in its unbound form and binds PP1, through a folding-upon-binding mechanism, in an elongated fashion, blocking one of PP1's three putative substrate binding sites, without altering its active site. This mode of binding is sufficient for spinophilin to restrict PP1's activity toward a model substrate *in vitro*, without affecting its ability to dephosphorylate its neuronal substrate GluR1. Thus, our work provides the molecular basis for the ability of spinophilin to dictate PP1 substrate specificity.

Keywords

serine/threonine signaling; Protein Phosphatase 1; PP1; intrinsically unstructured protein; spinophilin

Correspondence should be addressed to W.P. (wolfgang_peti@brown.edu).

Accession Codes

Atomic coordinates and structure factors for the reported crystal structures have been deposited with the Protein Data Bank under accession codes 3EGG (spinophilin:PP1), 3EGH (spinophilin:PP1:nodularin-R) and 3HVQ (neurabin:PP1). Chemical shifts of spinophilin$_{417\text{-}494}$ were deposited in the BMRB as entry 15180.

Supplementary information

Supplementary information is available on the Nature Structural & Molecular Biology website.

Author Contributions M.J.R. performed ITC, dephosphorylation assays, and crystallization of the spinophilin:PP1, spinophilin:PP1:nodularin-R and neurabin:PP1 complexes; W.P. purified unbound spinophilin for NMR studies B.D. performed and analyzed NMR studies of unbound spinophilin; M.J.R., D.A.C., and R.P. collected, processed and refined X-ray data; M.J.R., A.C.N., R.P. and W.P. wrote the paper. All authors discussed the data and manuscript. The authors declare that they have no competing financial interests.

INTRODUCTION

Transient protein modification is an essential regulatory mechanism for many biological processes. One type of transient modification, phosphorylation, is predicted to occur on approximately 1/3 of the total proteins encoded within the human genome[1,2]. In most eukaryotes, the number of enzymes responsible for the phosphorylation (kinases) and dephosphorylation (phosphatases) of tyrosine residues are nearly identical, ensuring high specificity of their critical functions[3]. However, the ratio of human Ser/Thr kinases to phosphatases is well in favor of the kinases (428:~40). Since the majority of Ser/Thr phosphorylation sites are reversible, the specificity of the phosphatases appears to be low when compared to Ser/Thr kinases.

Protein Phosphatase 1 (PP1) is the most widely expressed and abundant Ser/Thr phosphatase. PP1 is a single domain protein that is exceptionally well conserved from fungi to human, in both sequence and function. Dephosphorylation events by PP1 regulate cell cycle progression, protein synthesis, muscle contraction, carbohydrate metabolism, transcription and, of specific interest for this work, neuronal signaling[4]. The structure of apo-PP1 is not known, largely due to its high instability in solution[5]. However, the structure of PP1 bound to tungstate[6] or various PP1 inhibitors[5,7,8] shows that the catalytic site of PP1, which contains two metal ions, is at the intersection of three putative substrate binding regions, referred to as the hydrophobic, acidic and C-terminal grooves.

While the specificity of Ser/Thr phosphatases appears low, PP1 is nevertheless able to dephosphorylate its numerous targets with high specificity. To achieve this specificity, PP1 interacts with a large number of regulatory proteins (~200 confirmed interactors)[9]. PP1 regulatory proteins include inhibitory proteins that keep PP1 in an inactive state and targeting proteins that form highly specific holo-enzymes[10]. Targeting proteins direct the specificity of PP1 by localizing it to its point of action within the cell, as well as by directly altering its substrate preferences[4].

Most PP1-regulatory proteins (≥95%) contain a primary PP1 binding motif (R/K)(R/K)(V/I)×(F/W), commonly referred to as the RVxF motif, which interacts with a binding region more than 20 Å away from the active site of PP1[4,11]. A structure of PP1 with an RVxF peptide has been described[12], however it provided only limited insights into the regulation of PP1, as this interaction seems to be identical for all PP1 complexes. There is a limited number of holoenzyme structures currently available, due to the instability of apo-PP1 in solution[5] and the high flexibility of most PP1 regulatory proteins[13], which makes crystallography exceedingly challenging. Only a single structure of an inhibitor:PP1 (inhibitor-2:PP1[14]) and a targeting protein:PP1 (MYPT1 regulatory subunit:PP1[15]) complex have been reported. While these structures provide the first insights into the regulation of PP1, a detailed understanding of the molecular basis for the ability of targeting proteins to direct the substrate specificity of PP1 is still not understood.

To this end, we have used a combination of NMR (nuclear magnetic resonance) spectroscopy, x-ray crystallography and biochemistry to elucidate how spinophilin, the most extensively studied neuronal PP1 targeting protein, binds and directs PP1 substrate

specificity. Spinophilin, an 817 residue neuronal regulatory protein (Fig. 1a), targets PP1 to neuronal synapses[16] where it controls essential neuronal processes including AMPA receptor activation[17] and cytoskeletal reorganization[18],[19], and therefore plays a decisive role in learning and memory formation. Furthermore, spinophilin has been shown to play an important role in the actions of drugs of abuse[19],[20], and changes in PP1 function have been associated with Parkinson's disease[21]. Here, we show that the PP1 binding domain of spinophilin is highly dynamic in its unbound state. We also show this flexibility enables spinophilin to interact with PP1 over an extensive surface, forming many unexpected interactions. These results reveal a novel mechanism for the regulation of PP1 substrate specificity, where spinophilin binds to PP1 and blocks one of three potential PP1 substrate binding grooves without altering its active site. This work provides fundamental new insights into the regulation of the substrate specificity of PP1 at the molecular level.

RESULTS

The spinophilin PP1-domain is an unstructured peptide in solution

It was previously shown that the PP1 binding domain of spinophilin, residues 417-494 (spinophilin$_{417-494}$), is necessary and sufficient for its complete interaction with PP1[22]. Using NMR spectroscopy, we investigated the three dimensional structure of unbound spinophilin$_{417-494}$ and demonstrated that it is highly dynamic in solution. A 2D [^{1}H,^{15}N] HSQC (heteronuclear single quantum coherence) spectrum of spinophilin$_{417-494}$ contained little chemical shift dispersion in the $^{1}H^{N}$ dimension and amino acid specific clustering in the ^{15}N dimension, indicative of a highly flexible unstructured domain, commonly referred to as an intrinsically disordered protein (Fig. 1b)[23]. In addition, this flexibility was not altered when associated with its C-terminal structured PDZ domain (spinophilin$_{417-602}$; Fig. 1c).

Carbon chemical shifts, ^{15}N auto-correlated relaxation measurements and paramagnetic relaxation enhancements (PREs) were measured to test for potential preferred secondary structures or a preferred 3-dimensional topology. However, in marked contrast to our studies of PP1 inhibitors[13], the other class of PP1 regulatory molecules, it was not possible to identify any preferred secondary structures or a preferred 3-dimensional topology for unbound spinophilin$_{417-494}$ (Fig. 1d,e). Taken together, these data directly show that spinophilin$_{417-494}$ resembles a random-coil polypeptide in solution.

Nevertheless, the unstructured spinophilin PP1-binding domain is functional and interacts strongly with PP1 (α-isoform was used for all studies here). Isothermal titration calorimetry (ITC) measurements using spinophilin$_{417-583}$ and our recombinant PP1 indicated a dissociation constant (K_d) of 8.7 nM (Fig. 2a), which agrees well with data available for the interaction of spinophilin with PP1 from natural source[22]. Thus, our recombinant spinophilin and PP1 preparations behave similarly to endogenous proteins, confirming that the data reported here reflect the biologically relevant holo-enzyme (spinophilin$_{417-583}$:PP1 complex).

The crystal structure of the spinophilin:PP1 holoenzyme

In order to elucidate how spinophilin directs PP1 substrate specificity at a molecular level, we determined the 1.85 Å crystal structure of the complex between spinophilin$_{417-583}$ and PP1α$_{7-330}$ (Fig. 2b, Supplementary Fig. 1, Table 1). The overall structure of PP1 is essentially identical to reported PP1 structures[7],[24]. The catalytic site of PP1 is at the intersection of three potential substrate binding regions, referred to as the hydrophobic, acidic and C-terminal grooves. Two metal ions (Mn^{2+} in the recombinant protein, as the protein was expressed in LB medium supplemented with $MnCl_2$, but likely Fe^{2+} and Zn^{2+} in native PP1[7]) that are essential for the catalytic activity of PP1 are present in the active site of the spinophilin:PP1 holo-enzyme. The PP1 binding domain of spinophilin, which is unstructured when not bound to PP1, becomes restricted to a single conformation with residues 424-489 visible in both molecules of the asymmetric unit (Fig. 2c, Supplementary Fig. 1). Thus, the spinophilin PP1-binding domain entirely folds upon binding to PP1. We also determined the 3-dimensional structure of the neurabin:PP1 holo-enzyme (Supplementary Fig. 2; Supplementary Table 1). Neurabin is the neuron specific isoform of spinophilin (neurabin-II) and spinophilin and neurabin have ~80% identical primary sequence. No major differences were observed between the two 3-dimensional structures.

Strikingly, spinophilin$_{417-583}$ interacts with PP1 in an unexpected and unique manner, occupying not just the RVxF motif binding pocket (Fig. 3a), but also forming multiple interactions with different regions of PP1 including a substantial part of the PP1 C-terminal groove. The highly dynamic nature of spinophilin in its unbound state is likely essential for forming the substantial intermolecular interface of 3926 Å^2 between spinophilin and PP1[25], ~2.5 times larger than the average interface for protein:protein complex[26], and burying ~16% of the surface of the globular catalytic domain of PP1.

Spinophilin binds PP1 at multiple regions

The interaction of spinophilin with PP1 can be divided into four unique regions. Region I is formed by spinophilin residues 447-451 (RKIHF, the RVxF motif), which interact in the PP1 RVxF binding groove (Fig. 3a,b); this is the only expected interaction, based on previous work. As seen in the MYPT1 regulatory subunit:PP1[15] and inhibitor-2:PP1[14] complex structures, residues of the spinophilin RVxF motif bind in an extended conformation with spinophilin residues Ile$_{449}$ and Phe$_{451}$ buried in the PP1 RVxF binding groove. However, in contrast to all previously described interactions, the histidine residue at position ‘x’ of the spinophilin RVxF motif forms a hydrogen-bond with Thr$_{288}$ in PP1. In neurabin the residue occupying the ‘x’ position is a lysine, which also forms an identical polar contact with PP1 (Supplementary Fig. 3a). This indicates that for both the spinophilin:PP1 and neurabin:PP1 holoenzymes, the residue at position ‘x’ unexpectedly plays a role in the RVxF motif binding interaction.

Interaction regions II and III of spinophilin undergo what is commonly referred to as “coupled folding and binding”[27] (Fig. 2c). In region II, spinophilin residues 430-434 and 456-460 fold to form two β-strands which extend the PP1 β-sheet 1 into an extensive 7-strand β-sheet (Figs. 2b,c and 4a). In region III, spinophilin residues 476-492 fold into a 4-turn α-helix that forms electrostatic and hydrophobic interactions with the surface of PP1,

and is adjacent to both the C-terminal and hydrophobic grooves (Figs. 2b,c and 4b). Both the β-strands and α-helix were not observed in unbound spinophilin and thus require PP1 to fold.

Region IV is formed by spinophilin residues 462-469, which bind into a substantial part of the PP1 C-terminal groove (Figs. 2b,c and 4c; Supplementary Fig. 3b for neurabin). Here, spinophilin Arg_{469}, which has the second highest buried surface area of any spinophilin residue (only Ile_{449} of the RVxF motif is greater), forms the core of this interaction. It does so by establishing strong backbone and sidechain hydrogen-bond interactions both intramolecularly, with Tyr_{462} and Asn_{464} in spinophilin, and intermolecularly with Asp_{71} in PP1. These interactions prime spinophilin residues Tyr_{462} and Tyr_{467} to form extensive hydrophobic interactions with PP1.

To understand the influence of each of the four spinophilin:PP1 interaction regions, we created multiple single mutants of the spinophilin PP1 binding domain and measured their ability to influence binding to PP1. None of the introduced mutations disrupt the overall fold of spinophilin, as indicated by circular dichroism spectrum analysis (Supplementary Fig. 4). As shown in Fig. 5a,b the mutations that most negatively impacted PP1 binding are residues in the spinophilin RVxF motif (interaction region I, F451A) and the C-terminal groove binding motif (interaction region IV, Y467A, R469A, R469D), with a smaller negative effect observed for residues in the β-sheet area (interaction region II, F459A). Notably, the hydrophobic Phe residue in the RVxF motif (F451) had the most negative effect on PP1 binding, in excellent agreement with the reported RVxF motif mutational analysis of other regulator:PP1 complexes[9,12]. Interestingly, single point mutations in the α-helix had the least influence on PP1-binding.

Spinophilin does not affect the binding of molecules at the active site of PP1

Despite its extensive interaction surface spinophilin does not bind PP1 near its active site and appears to leave the active site unchanged. We verified this by determining the 2.0 Å crystal structure of the spinophilin:PP1:nodularin-R triple complex. Nodularin-R is a molecular toxin that inhibits PP1 by direct active site interaction[5]. Comparison of this structure with the PP1:nodularin-R co-complex structure (PDBID 3E7A)[5] reveals that spinophilin does not alter the binding interactions of molecules directly at the active site of PP1, nor does it alter the PP1 hydrophobic substrate binding groove (Fig. 5c and Supplementary Fig. 5).

The extensive spinophilin:PP1 interactions define the specificity of PP1

Despite the fact that the interaction of molecules at the active site of PP1 is unchanged, spinophilin directs PP1 substrate specificity in a manner independent of its ability to target PP1 to distinct subcellular locations, a phenomenon which has also been described for other PP1 targeting proteins[12,28]. This is shown in Figure 5d, which illustrates the decisively altered dephosphorylation efficiency of PP1 in the presence and absence of $spinophilin_{417\text{-}583}$. The PP1 substrates used were: 1) Ser845-protein kinase A (PKA) phosphorylated $GluR1_{809\text{-}889}$, a specific substrate of the spinophilin:PP1 holo-enzyme[17] ($GluR1_{809\text{-}889}$); 2) phosphorylase *a*, a specific substrate of the GM:PP1 holo-enzyme and

not the spinophilin:PP1 holo-enzyme[29]; and 3) *p*-nitrophenyl phosphate (*p*NPP), a commonly used model substrate. Spinophilin inhibits the activity of PP1 for phosphorylase *a* (red) while it has no effect on the activity of PP1 for GluR1 (blue) and *p*NPP (green). Interestingly, this inhibition can be completely ablated by a mutation of either spinophilin Phe_{451} or Arg_{469} (Fig. 5d), clearly showing that both interactions are necessary for the formation of the functional holo-enzyme. The unaltered dephosphorylation efficiency of PP1 for the small molecule substrate *p*NPP lends further support to the observation that spinophilin does not alter the binding of molecules at the active site of PP1. Therefore, the striking change in substrate specificity of the spinophilin:PP1 holo-enzyme must result from a modification of the PP1 substrate binding surface. This can be achieved by either an alteration of the surface electrostatics, by steric blocking of essential binding sites, or both.

Although the interaction surface between PP1 and spinophilin is extensive, spinophilin binding does not substantially alter the charge distribution of the enzyme (Fig. 5e). Instead, spinophilin directs PP1 specificity by a novel mechanism, via steric inhibition of alternative substrate binding sites. Spinophilin binds to a large part of the PP1 C-terminal groove, blocking access to substrates that require this groove for binding to PP1. Indeed, mutation of Asp_{71} (Fig. 4c), a PP1 residue located in the center of the C-terminal substrate binding pocket, led to a substantial increase in the K_M for dephosphorylation of phosphorylase *a*[30], highlighting its role in substrate binding. In the spinophilin:PP1 holo-enzyme, Asp_{71} forms a hydrogen bond with spinophilin Arg_{469} and is completely inaccessible to solvent. To further investigate the role of Asp_{71} in substrate selectivity we have tested the activity of PP1 D71N against phosphorylated $GluR1_{809\text{-}889}$ and phosphorylase *a* (Fig. 5f). We found the expected decrease by a factor of 3.0 in the activity of PP1 for phosphorylase *a*, identical to the decrease by a factor of 2.9 that we identify when using the spinophilin:PP1 holoenzyme. However, mutation of D71 had no effect on the dephosphorylation of $GluR1_{809\text{-}889}$. Further corroborating these results, spinophilin shows ~60% reduced binding to PP1 D71N (Fig. 5g). Lastly, the only interaction region with 100% primary sequence identity between the isoforms neurabin and spinophilin is the amino acid sequence required for binding to the PP1 C-terminal groove, further highlighting the importance of this interaction.

DISCUSSION

Our biochemical, dynamic and structural data of the spinophilin PP1-binding domain alone and the sphinophilin:PP1 holoenzyme demonstrates that spinophilin is an intrinsically unstructured protein that undergoes a folding-upon-binding transition upon interaction with PP1. The high intrinsic flexibility of unbound spinophilin allows for unique interactions with PP1 resulting in an unusually large protein:protein interface. Spinophilin binds, as anticipated, into the PP1 RVxF binding groove. However, surprisingly, spinophilin also binds PP1 in numerous additional surface grooves, including the C-terminal substrate binding groove. While the spinophilin RVxF motif is critical for PP1 binding, residues that interact with the PP1 β-strands, as well as the PP1 C-terminal groove are also important, with the latter interaction region necessary for directing the substrate specificity of PP1.

Taken together, these structural and biochemical data provide a novel explanation for the reduced dephosphorylation efficiency of the spinophilin:PP1 holo-enzyme for

phosphorylase *a*. The results clearly show the importance of the interaction of spinophilin with the PP1 C-terminal binding groove for altering the substrate specificity of PP1. Based on this data we propose that apo-PP1 is able to bind substrates using any combination of its three potential substrate binding grooves (Fig. 6a). Importantly, spinophilin binds into only one of these three alternative sites, thus the acidic and hydrophobic substrate binding grooves are still accessible. However in the presence of spinophilin, PP1 can only bind, and, in turn, select substrates that interact with either the hydrophobic and/or acidic grooves (Fig. 6b); substrates that require the C-terminal groove for substrate binding, such as phosphorylase *a* are blocked. This mechanism for altered substrate specificity of PP1 is different to that reported for the MYPT1:PP1 holo-enzyme, which was proposed to be driven by altered electrostatics[15]. However, also when MYPT1 binds to PP1, a modified substrate binding surface, with extended substrate grooves is formed (Supplementary Fig. 6). Taking the data from these two structures it is likely that PP1 can achieve substrate specificity via a substrate exclusion process, which is exemplified by spinophilin:PP1, as well as by a combined substrate inclusion-exclusion process, which is exemplified by MYPT1:PP1.

In addition, this is the first time, to our knowledge, that an intrinsically disordered protein (spinophilin) has been shown to regulate enzymatic activity by directing the substrate specificity of an enzyme instead of activating or inhibiting it directly. While the PP1-binding domain of spinophilin behaves as a random coil peptide in solution, it completely folds upon binding to PP1 and becomes rigid. The results obtained here, taken together with the targeting of spinophilin:PP1 to the post-synaptic aspect of the synapse, will ensure that PP1 is placed in an active state close to its selected substrate, GluR1.

Further comparison of the spinophilin:PP1 holo-enzyme structure with the two previously reported regulatory protein:PP1 holo-enzymes (inhibitor-2:PP1, Mypt1:PP1) shows that the binding mode for all three proteins is unique and that the only shared interaction is the conserved RVxF binding groove[14],[15]. Thus, this comparison, combined with other biochemical data[31], strongly suggests that nearly every accessible surface on the catalytic face of PP1 is a potential protein interaction site, allowing for numerous unique interactions and therefore abundant unique holo-enzymes, each with individual substrate preferences. These observations begin to explain the striking diversity of PP1 holo-enzymes, each of which may form a truly unique enzyme with distinctive properties. This is made even more intriguing by the fact that the number (~200) of identified PP1 targeting proteins is still increasing[9]. If the diversity of interactions observed for PP1 is conserved across ser/thr phosphatases, it would allow the ~40 ser/thr phosphatases to form hundreds of unique holo-enzymes, ensuring that they are as specific as the 428 known ser/thr kinases.

Methods

The methods and their associated references appear only online.

Supplementary Material

Refer to Web version on PubMed Central for supplementary material.

Acknowledgments

This work was supported by NIH (NS056128 to WP; MH074866 to ACN). WP is the Manning Assistant Professor of Medical Science at Brown University. This material is based upon work supported under a National Science Foundation Graduate Research Fellowship to B.D. Crystallographic data was collected at the X6A beam line, funded by the National Institute of General Medical Sciences, under agreement GM-0080. The National Synchrotron Light Source, Brookhaven National Laboratory is supported by the U.S. Department of Energy under contract number DE-AC02-98CH10886.

References

1. Ubersax JA, Ferrell JE Jr. Mechanisms of specificity in protein phosphorylation. Nat Rev Mol Cell Biol. 2007; 8:530–41. [PubMed: 17585314]
2. Cohen P. The regulation of protein function by multisite phosphorylation--a 25 year update. Trends Biochem Sci. 2000; 25:596–601. [PubMed: 11116185]
3. Alonso A, et al. Protein tyrosine phosphatases in the human genome. Cell. 2004; 117:699–711. [PubMed: 15186772]
4. Cohen PT. Protein phosphatase 1--targeted in many directions. J Cell Sci. 2002; 115:241–56. [PubMed: 11839776]
5. Kelker MS, Page R, Peti W. Crystal structures of protein phosphatase-1 bound to nodularin-R and tautomycin: a novel scaffold for structure-based drug design of serine/threonine phosphatase inhibitors. J Mol Biol. 2009; 385:11–21. [PubMed: 18992256]
6. Egloff MP, Cohen PT, Reinemer P, Barford D. Crystal structure of the catalytic subunit of human protein phosphatase 1 and its complex with tungstate. J Mol Biol. 1995; 254:942–59. [PubMed: 7500362]
7. Goldberg J, et al. Three-dimensional structure of the catalytic subunit of protein serine/threonine phosphatase-1. Nature. 1995; 376:745–53. [PubMed: 7651533]
8. Maynes JT, et al. Crystal structure of the tumor-promoter okadaic acid bound to protein phosphatase-1. J Biol Chem. 2001; 276:44078–82. [PubMed: 11535607]
9. Hendrickx A, et al. Docking motif-guided mapping of the interactome of protein phosphatase-1. Chem Biol. 2009; 16:365–71. [PubMed: 19389623]
10. Ceulemans H, Bollen M. Functional diversity of protein phosphatase-1, a cellular economizer and reset button. Physiol Rev. 2004; 84:1–39. [PubMed: 14715909]
11. Bollen M. Combinatorial control of protein phosphatase-1. Trends Biochem Sci. 2001; 26:426–31. [PubMed: 11440854]
12. Egloff MP, et al. Structural basis for the recognition of regulatory subunits by the catalytic subunit of protein phosphatase 1. Embo J. 1997; 16:1876–87. [PubMed: 9155014]
13. Dancheck B, Nairn AC, Peti W. Detailed Structural Characterization of Unbound Protein Phosphatase 1 Inhibitors. Biochemistry. 2008; 47:12346–12356. [PubMed: 18954090]
14. Hurley TD, et al. Structural basis for regulation of protein phosphatase 1 by inhibitor-2. J Biol Chem. 2007; 282:28874–83. [PubMed: 17636256]
15. Terrak M, Kerff F, Langsetmo K, Tao T, Dominguez R. Structural basis of protein phosphatase 1 regulation. Nature. 2004; 429:780–4. [PubMed: 15164081]
16. Allen PB, Ouimet CC, Greengard P. Spinophilin, a novel protein phosphatase 1 binding protein localized to dendritic spines. Proc Natl Acad Sci U S A. 1997; 94:9956–61. [PubMed: 9275233]
17. Yan Z, et al. Protein phosphatase 1 modulation of neostriatal AMPA channels: regulation by DARPP-32 and spinophilin. Nat Neurosci. 1999; 2:13–7. [PubMed: 10195174]
18. Bielas SL, et al. Spinophilin facilitates dephosphorylation of doublecortin by PP1 to mediate microtubule bundling at the axonal wrist. Cell. 2007; 129:579–91. [PubMed: 17482550]
19. Charlton JJ, et al. Multiple actions of spinophilin regulate mu opioid receptor function. Neuron. 2008; 58:238–47. [PubMed: 18439408]
20. Allen PB, et al. Distinct roles for spinophilin and neurabin in dopamine-mediated plasticity. Neuroscience. 2006; 140:897–911. [PubMed: 16600521]

21. Brown AM, Baucum AJ, Bass MA, Colbran RJ. Association of protein phosphatase 1 gamma 1 with spinophilin suppresses phosphatase activity in a Parkinson disease model. J Biol Chem. 2008; 283:14286–94. [PubMed: 18372251]
22. Hsieh-Wilson LC, Allen PB, Watanabe T, Nairn AC, Greengard P. Characterization of the neuronal targeting protein spinophilin and its interactions with protein phosphatase-1. Biochemistry. 1999; 38:4365–73. [PubMed: 10194355]
23. Dyson HJ, Wright PE. Intrinsically unstructured proteins and their functions. Nat Rev Mol Cell Biol. 2005; 6:197–208. [PubMed: 15738986]
24. Kita A, et al. Crystal structure of the complex between calyculin A and the catalytic subunit of protein phosphatase 1. Structure. 2002; 10:715–24. [PubMed: 12015153]
25. Fraczkiewicz R, Braun W. Exact and Efficient Analytical Calculation of the Accessible Surface Areas and Their Gradients for Macromolecules. J Comp Chem. 1998; 19:319–333.
26. Lo Conte L, Chothia C, Janin J. The atomic structure of protein-protein recognition sites. J Mol Biol. 1999; 285:2177–98. [PubMed: 9925793]
27. Dyson HJ, Wright PE. Coupling of folding and binding for unstructured proteins. Curr Opin Struct Biol. 2002; 12:54–60. [PubMed: 11839490]
28. Tanaka J, et al. Interaction of myosin phosphatase target subunit 1 with the catalytic subunit of type 1 protein phosphatase. Biochemistry. 1998; 37:16697–703. [PubMed: 9843438]
29. Hubbard MJ, Cohen P. Regulation of protein phosphatase-1G from rabbit skeletal muscle. 2. Catalytic subunit translocation is a mechanism for reversible inhibition of activity toward glycogen-bound substrates. Eur J Biochem. 1989; 186:711–6. [PubMed: 2558014]
30. Zhang J, Zhang Z, Brew K, Lee EY. Mutational analysis of the catalytic subunit of muscle protein phosphatase-1. Biochemistry. 1996; 35:6276–82. [PubMed: 8639569]
31. Ceulemans H, et al. Binding of the concave surface of the Sds22 superhelix to the alpha 4/alpha 5/alpha 6-triangle of protein phosphatase-1. J Biol Chem. 2002; 277:47331–7. [PubMed: 12226088]
32. McCoy AJ, Grosse-Kunstleve RW, Storoni LC, Read RJ. Likelihood-enhanced fast translation functions. Acta Crystallogr D Biol Crystallogr. 2005; 61:458–64. [PubMed: 15805601]
33. Emsley P, Cowtan K. Coot: model-building tools for molecular graphics. Acta Crystallogr D Biol Crystallogr. 2004; 60:2126–32. [PubMed: 15572765]
34. Murshudov GN, Vagin AA, Dodson EJ. Refinement of Macromolecular Structures by the Maximum-Likelihood Method. Acta Crystallogr D. 1997; 53:240–255. [PubMed: 15299926]
35. Lamzin VS, Wilson KS. Automated refinement of protein models. Acta Crystallogr D Biol Crystallogr. 1993; 49:129–47. [PubMed: 15299554]
36. Painter J, Merritt EA. TLSMD web server for the generation of multi-group TLS models. J Appl Cryst. 2006; 39:109–111.
37. Davis IW, et al. MolProbity: all-atom contacts and structure validation for proteins and nucleic acids. Nucleic Acids Res. 2007; 35:W375–83. [PubMed: 17452350]
38. Laskowski RA, MacArthur MW, Moss DS, Thornton JM. PROCHECK: a program to check the stereochemical quality of protein structures. J Appl Cryst. 1993; 26:283–291.
39. Cohen P, et al. Protein phosphatase-1 and protein phosphatase-2A from rabbit skeletal muscle. Methods Enzymol. 1988; 159:390–408. [PubMed: 2842604]
40. Jacques AM, et al. Myosin binding protein C phosphorylation in normal, hypertrophic and failing human heart muscle. J Mol Cell Cardiol. 2008; 45:209–16. [PubMed: 18573260]

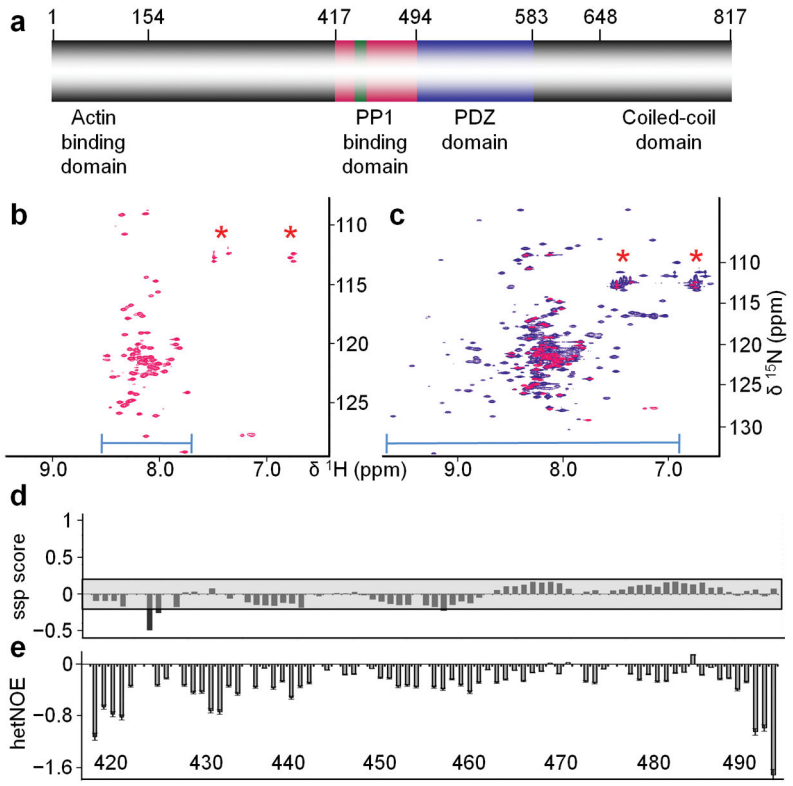

Figure 1.

The unbound spinophilin PP1-binding domain. (a) Domain structure map of spinophilin with the conserved RVxF motif highlighted in green, the PP1 binding domain in magenta and the PDZ domain in purple (color codes are constant throughout all figures). (b) 2D [1H, 15N] HSQC spectrum of spinophilin417-494. The blue bar highlights the lack of dispersion for the chemical shifts in the 1HN dimension. (c) An overlay of the 2D [1H,15N] HSQC spectra of spinophilin417-602 (purple) and spinophilin417-494 (magenta). The blue bar highlights the larger dispersion for the chemical shifts in the 1HN dimension resulting from the well ordered PDZ domain while the chemical shifts of spinophilin417-494 remain unchanged. Red asterisks indicate side chain NH2 groups of Asn and Gln. (d) Ssp scores and (e) 15N[1H]-NOE (hetNOE) data are plotted against spinophilin residue numbers. These data indicate that there are no regions of transient structure nor reduced backbone motions in spinophilin417-494. Also, no areas of considerably populated transient secondary structure were detected. Regions of considerably populated transient structure were considered five residues or more with an ssp score > 0.2, indicating a transient α-helix, or < −0.2, indicating a region with extended structure (not considerably populated regions are indicted by a gray box).

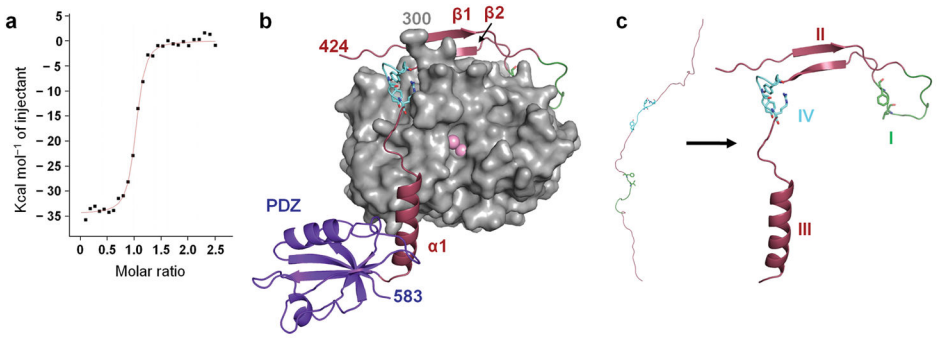

Figure 2.

The spinophilin417-583:PP1α7-330 complex. (a) Isothermal titration calorimetry of purified spinophilin417-583 and PP1α7-330 yielding a Kd of 8.7 nM and confirming that the intrinsically unstructured spinophilin PP1-binding domain is active. (b) Cartoon representation of the spinophilin417-583 PP1 binding (magenta) and PDZ domains (purple) and PP1α7-330 (gray; surface representation) complex; centered on the active site of PP1α7-330. Two Mn2+-ions (pink spheres) mark the active site of PP1. The newly formed secondary structure elements of spinophilin417-494 are labeled β1, β2 and α1. The PDZ domain is C-terminal to α1 and is labeled PDZ. Spinophilin residues interacting with the RVxF binding pocket are represented as sticks in green and those interacting with the PP1 C-terminal groove are represented as sticks in cyan. (c) The spinophilin PP1-binding domain before (unstructured model, left) and after binding to PP1 (crystal structure without PP1, right), illustrating the unfolded-to-folded transition. The four unique regions that characterize the interaction of spinophilin (magenta) with PP1 are numbered; RVxF (green); C-terminal groove binding motif (cyan).

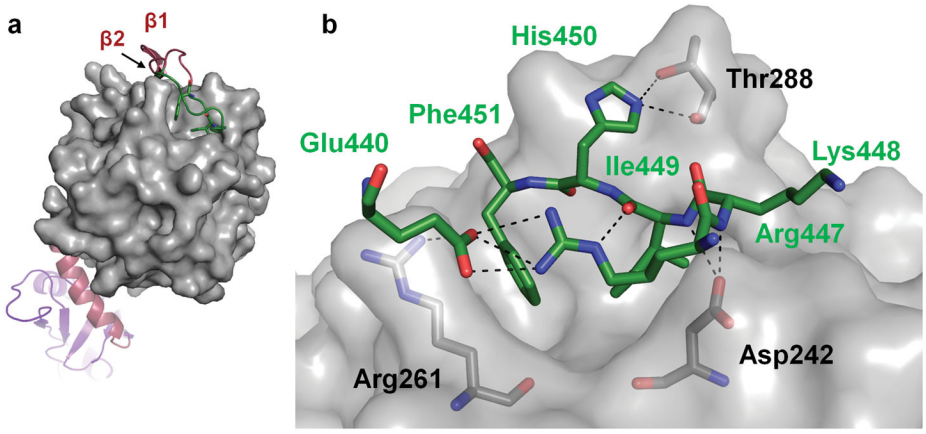

Figure 3.

Spinophilin's interaction with the PP1 RVxF binding pocket. (a) 90o rotation of Fig. 2b to highlight the interaction of Ile449 and Phe451 in the RVxF binding pocket. (b) Spinophilin residues (RVxF sequence, green) and PP1 (gray, surface and stick representation for interacting residues) are shown with oxygen atoms in orange and nitrogen atoms in dark blue. Hydrogen bonds are represented as black dashes. The spinophilin RVxF sequence (447RKIHF451) is preceded by a long loop which folds back on itself (Fig. 2b,c) to form a strong hydrogen bond network. Some residues in the loop have been omitted for clarity.

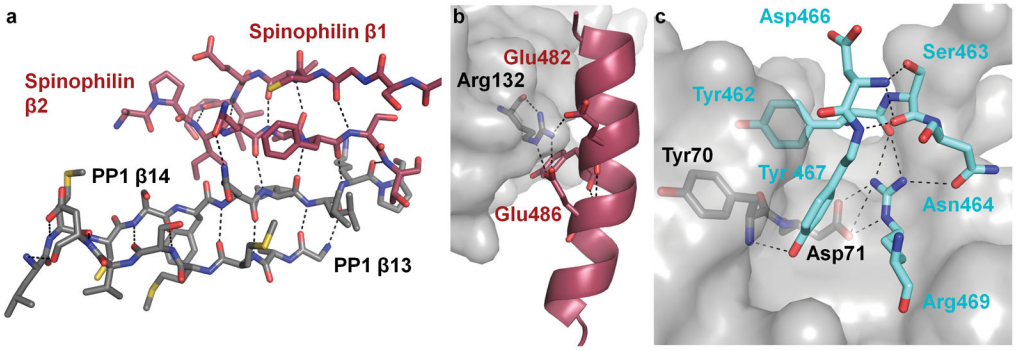

Figure 4.

Spinophilin's PP1 interaction regions II, III and IV. (a) Region II: Spinophilin forms two novel β-strands upon binding to PP1. Stick representation of spinophilin residues 428-435 (β1 includes residues 430-434) and 454-461 (β2 includes residues 456-460) which form an extended β-sheet with the strands β13 and β14 of PP1. (b) Region III: Spinophilin forms a 4-turn α-helix upon interaction with PP1. View of the helix highlighting electrostatic and hydrophobic interaction clusters between the helix and the surface of PP1. (c) Region IV: Spinophilin residues 462-469 interact directly with the C-terminal groove of PP1. These residues protrude directly into the binding pocket forming a complex hydrogen bonding network with both PP1 and within spinophilin. Spinophilin residues 465 and 468 have been omitted for clarity.

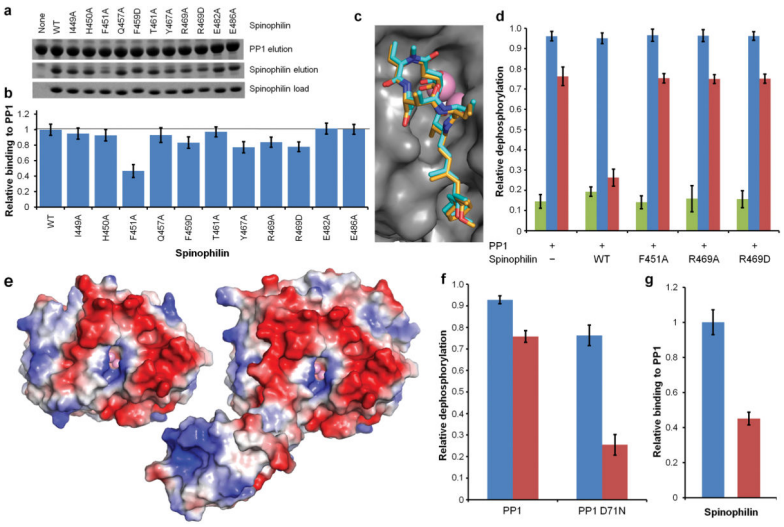

Figure 5.

Spinophilin creates a unique holoenzyme with novel substrate specificity. (a) The relative binding of spinophilin (mutants vs. WT; region I: I449A, H450A, F451A; region II: Q457A, F459D, T461A; region II: E482A, E486A; region IV: Y467A, R469A, R469D) to PP1α7-330 was determined using a capture assay. Elution fractions as well as all loaded spinophilin samples were subjected to SDS-PAGE gel electrophoresis analysis using Coomassie staining. (b) Densitometry was performed on the PP1 and spinophilin elutions to determine the amount of spinophilin that co-eluted with PP1α7-330. The experiment was repeated twice with error bars representing the standard deviation. (c) Overlay of the active site of spinophilin417-583:PP1α7-330:nodularin-R (orange) with PP1α7-330:nodularin-R (cyan; PDBID 3E7A). (d) PP1α7-330 dephosphorylation of various substrates in vitro: pNPP (green) GST-GluR1809-889 (blue) and phosphorylase a (red). Error bars represent standard deviations (n = 4). (e) Electrostatic surface representation (red: negative charge; blue: positive charge; grey: hydrophobic) of PP1α7-330 and spinophilin417-583:PP1α7-330 centered on the active site. (f) Mutation of PP1 Asp71 inhibits the dephosphorylation of phosphorylase a. PP1α7-330 (left) and PP1α7-330 D71N (right) dephosphorylation of GST-GluR1809-889 (blue) and phosphorylase a (red) in vitro. Error bars represent standard deviations (n = 4). (g) The PP1 D71N mutant reduces spinophilin binding by a factor of 2.2. WT-spinophilin to WT-PP1 (blue) and PP1 D71N mutant (red) was tested. Error bars represent standard deviations (n = 2).

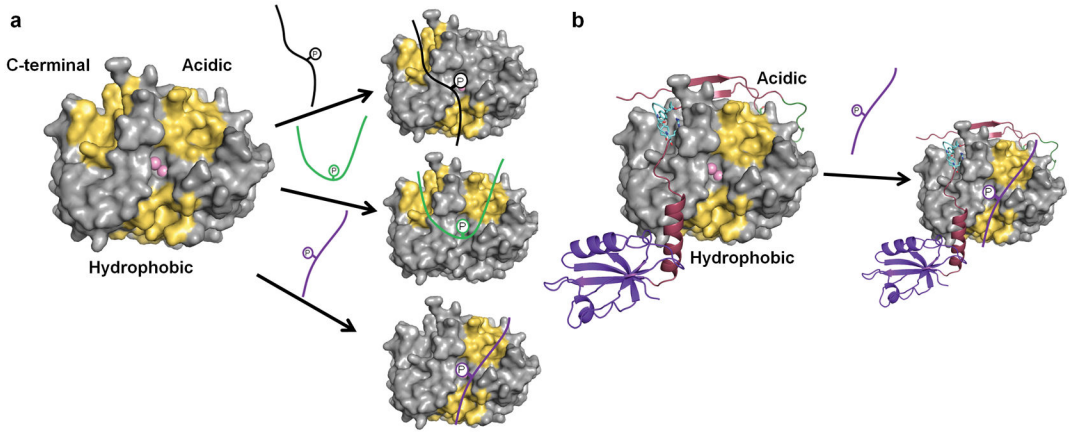

Figure 6.

Spinophilin affects the PP1 substrate binding surface without changing the active site. (a) Model for substrate recognition by apo-PP1. (b) Model for substrate recognition by the spinophilin:PP1 holoenzyme. The three PP1 substrate binding grooves are colored yellow. Potential substrates are shown as green, purple and black lines. Spinophilin achieves substrate specificity by steric exclusions of substrate binding sites.

Table 1

Data collection and refinement statistics for the spinophilin$_{417-583}$:PP1α$_{7-330}$ and the spinophilin$_{417-583}$:PP1α$_{7-330}$:Nodularin-R complex.

	Spinophilin$_{417-583}$:PP1α$_{7-330}$	**Spinophilin$_{417-583}$:PP1α$_{7-330}$:Nodularin-R**
Data collection		
Space group	C 2	C 2
Cell dimensions		
a, *b*, *c* (Å)	119.7, 84.4, 109.2	119.4, 84.4, 109.3
α, β, γ (°)	90.0, 93.5, 90.0	90.0, 93.6, 90.0
Resolution (Å)*	50.0-1.85 (1.88-1.85)	50.0-2.0 (2.07-2.00)
R_{merge}*	0.078 (0.596)	0.066 (0.281)
$I/\sigma I$*	10.9 (2.2)	13.6 (4.1)
Completeness (%)*	99.3 (97.9)	98.1 (82.5)
Redundancy*	3.7 (3.1)	3.6 (2.6)
Refinement		
Resolution (Å)	27.5 - 1.85	40.0 - 2.00
No. reflections	91551/4548	70101/3528
R_{work}/R_{free}	0.179/0.211	0.192/0.234
No. atoms		
Protein	6430	6372
Ligand/ion	4	113
Waters	521	481
B-factors		
Protein	25.6	29.6
Ligand/ion	22.0	29.3
Waters	33.0	35.9
R.m.s. deviations		
Bond lengths (Å)	0.011	0.015
Bond angles (°)	1.26	1.54

One crystal was used for each structure;

*Values in parentheses are for highest-resolution shell.